Photodissociation of laboratory oriented molecules: Revealing molecular frame properties of nonaxial recoil

van den Brom, A.J.; Rakitzis, T.P.; Janssen, M.H.M.

published in
Journal of Chemical Physics
2004

DOI (link to publisher)
10.1063/1.1812756

document version
Publisher's PDF, also known as Version of record

Photodissociation of laboratory oriented molecules: Revealing molecular frame properties of nonaxial recoil

Alrik J. van den Brom
Laser Centre and Department of Chemistry, Vrije Universiteit, de Boelelaan 1083, 1081 HV Amsterdam, The Netherlands

T. Peter Rakitzis
Department of Physics, University of Crete and IESL-FORTH, P.O. Box 1527, 71110 Heraklion, Greece

Maurice H. M. Janssen[a)]
Laser Centre and Department of Chemistry, Vrije Universiteit, de Boelelaan 1083, 1081 HV Amsterdam, The Netherlands

(Received 9 August 2004; accepted 14 September 2004)

We report the photodissociation of laboratory oriented OCS molecules. A molecular beam of OCS molecules is hexapole state-selected and spatially oriented in the electric field of a velocity map imaging lens. The oriented OCS molecules are dissociated at 230 nm with the linear polarization set at 45° to the orientation direction of the OCS molecules. The CO($\nu=0,J$) photofragments are quantum state-selectively ionized by the same 230 nm pulse and the angular distribution is measured using the velocity map imaging technique. The observed CO($\nu=0,J$) images are strongly asymmetric and the degree of asymmetry varies with the CO rotational state J. From the observed asymmetry in the laboratory frame we can directly extract the molecular frame angles between the final photofragment recoil velocity and the permanent dipole moment and the transition dipole moment. The data for CO fragments with high rotational excitation reveal that the dissociation dynamics is highly nonaxial, even though conventional wisdom suggests that the nearly limiting β parameter results from fast axial recoil dynamics. From our data we can extract the relative contribution of parallel and perpendicular transitions at 230 nm excitation. © *2004 American Institute of Physics.* [DOI: 10.1063/1.1812756]

I. INTRODUCTION

The measurement of photofragment angular and energy distributions has been an extremely valuable tool for the study of photodissociation dynamics. The angular dependence of the recoil distribution of photofragments after photolysis of an isotropic ensemble of parent molecules can be described by the following expression:[1]

$$I(\theta)=\frac{\sigma}{4\pi}[1+\beta P_2(\cos\theta)], \tag{1}$$

where θ is the laboratory frame angle between the linear polarization of the photolysis light $\vec{\epsilon}$ and the recoil velocity $\vec{v}$, σ is the integrated reaction cross section, β is the anisotropy parameter, and $P_2(\cos\theta)$ the second Legendre polynomial. The anisotropy parameter β ranges from -1 for a perpendicular transition to $+2$ for a parallel transition. Intermediate values may occur for various reasons, for instance the simultaneous excitation to two surfaces with different symmetry, a finite lifetime of the dissociating molecule comparable to the rotational period of the system, or an excitation where the transition dipole moment is neither parallel nor perpendicular to the recoil direction.[2–5] In the fast axial recoil approximation, it is assumed that recoil is fast on the time scale of rotation and that the asymptotic recoil velocity is directed along the initial orientation of the dissociated bond. Breakdown of this approximation occurs when the parent molecule rotates significantly during the dissociation[6] or when the dissociating potential energy surface is anisotropic. In the latter case, nonaxial forces during the dissociation may cause the fragments to acquire a significant tangential velocity producing a curved recoil trajectory. It is clear that in general the interpretation of a nonlimiting β parameter is not straightforward.

It has been discussed that, in principle, photodissociation experiments of laboratory oriented molecules will be able to disentangle the various underlying processes and that such experiments may potentially reveal more details of the molecular frame dynamics.[7–9] A few theoretical papers[10–12] discussed how in case of fast axial recoil the angular distribution of photofragments from the photodissociation of oriented molecules does not provide additional information on the dissociation dynamics beyond the β parameter. For fast axial recoil, the angular distribution of fragments can be written as the product of the orientational probability distribution of the parent molecule and the recoil distribution given in Eq. (1). This theoretical prediction was experimentally confirmed for the fast axial photodissociation of oriented methyl iodide.[13,14]

In this paper we report on the photodissociation at 230 nm of laboratory oriented OCS molecules producing CO(J) and S($^1D_2$) fragments. In previous studies[15–19] of randomly

a)Electronic mail: mhmj@chem.vu.nl

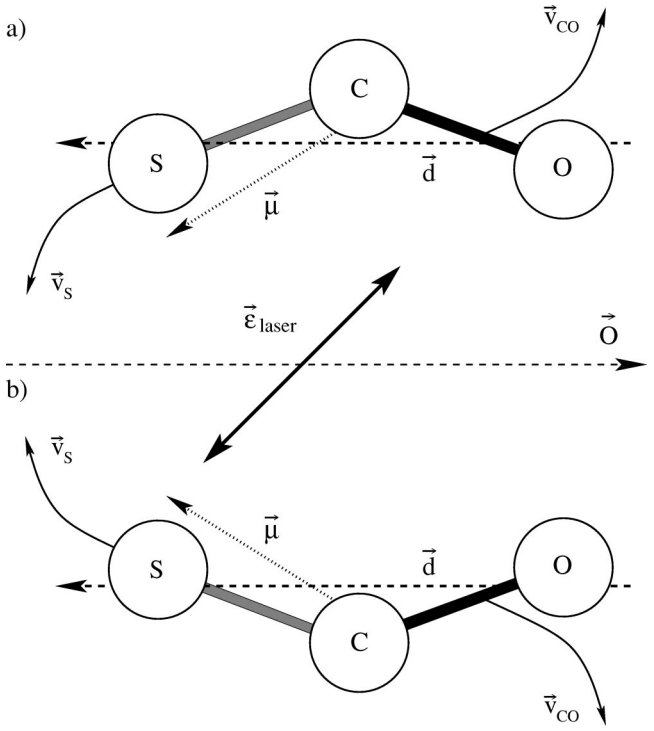

FIG. 1. The OCS molecules are oriented horizontally with the S atom towards the left. By setting the laser polarization at 45° with respect to the orientation axis, dissociation of OCS molecules oriented as in the upper half (a) of the figure is favored over dissociation of OCS molecules oriented as in the lower half (b). A nonzero angle between the asymptotic recoil velocity of the photofragments ($\vec{v}_S$ or $\vec{v}_{CO}$) and the permanent dipole $\vec{d}$ and the transition dipole $\vec{\mu}$ will lead to an up-down asymmetry in the laboratory frame recoil distribution.

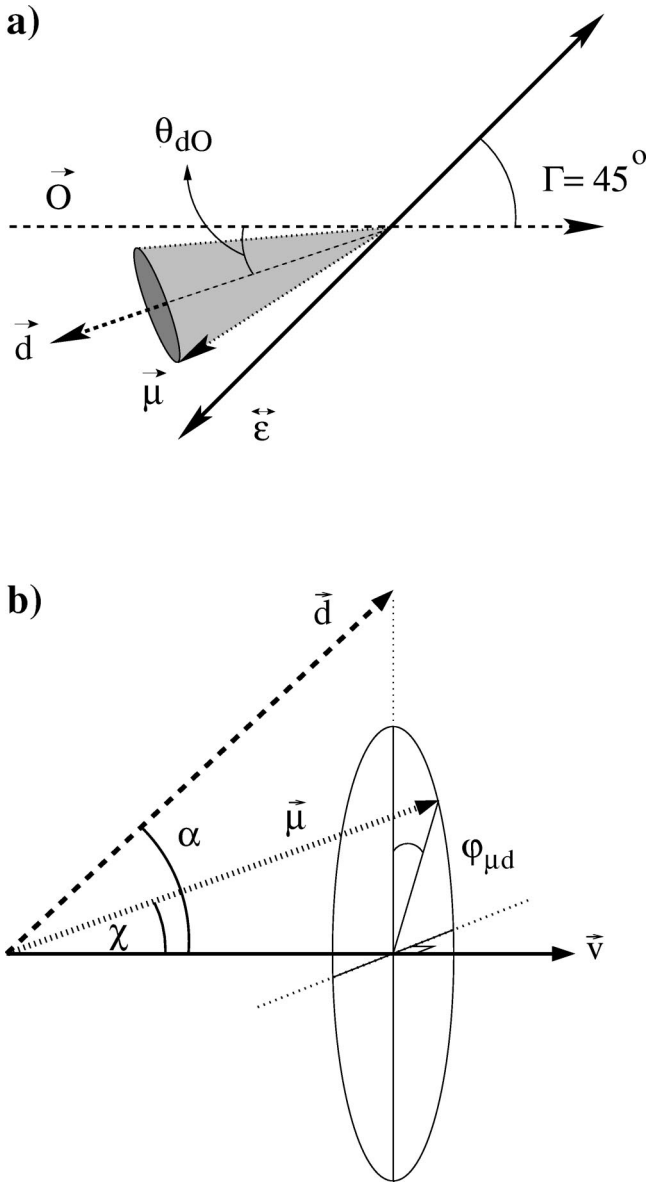

FIG. 2. (a) Orientation of the permanent dipole moment $\vec{d}$ and the transition dipole moment $\vec{\mu}$ with respect to the laboratory frame orientation direction $\vec{O}$, which has an angle $\Gamma=45°$ with the laser polarization $\vec{\epsilon}$. (b) Schematic picture of the direction of the permanent dipole moment $\vec{d}$ relative to the transition dipole moment $\vec{\mu}$ and the recoil velocity $\vec{v}$. The azimuthal angle $\varphi_{\mu d}$ rotates $\vec{\mu}$ about $\vec{v}$.

oriented parent molecules it was reported that for CO(J) in high rotational states the angular distribution is very parallel in character with $\beta \approx 1.8$, close to the limiting value of 2. This large β parameter suggests a fast axial recoil dynamics from a parallel excitation. However, it is known that for OCS, the transition to the repulsive excited states at 230 nm is symmetry forbidden when the molecule is linear. Bending of the linear parent molecule is required and strongly enhances the excitation.[17,19–21] The excited $1\,^1A''$ and $2\,^1A'$ dissociative surfaces are strongly anisotropic resulting in a nonaxial force excerted on the recoiling photofragments causing high rotational levels of the CO($X\,^1\Sigma^+, \nu=0, J$) photofragment $J \approx 45-68$ to be populated. The rotational state distribution shows a bimodal structure which was attributed to two physical processes.[17] The rotationally cold channel (J less than ≈ 57) is produced by a simultaneous excitation of both the $1\,^1A''$ and $2\,^1A'$ excited states, while the rotationally hot channel (J larger than ≈ 57) is produced by a pure parallel transition to the $2\,^1A'$ state, followed by a nonadiabatic transition to $1\,^1A'$ ground state. The first process results in a low value of β, whereas the second process results in a value of β much closer to $+2$. As the dissociating energy surfaces of OCS are strongly anisotropic the recoiling photofragments are directed away from the original orientation of the bond axis.

Recently, we reported the observation of a strong up-down asymmetry in the CO($J=62$) laboratory frame recoil distribution from the photodissociation of spatially oriented OCS.[22] It was shown how the dissociation dynamics in OCS is strongly nonaxial even though a near limiting β parameter is measured for high J states.[20] From the measured asymmetry we derived the photofragment deflection angle between the initial linear direction along the permanent dipole moment $\vec{d}$ and the final recoil velocity $\vec{v}$. To observe this asymmetry in the laboratory frame, the OCS parent molecules were oriented in an electric field $\vec{O}$ and the angle Γ between the orientation field and the laser polarization $\vec{\epsilon}$ was set at 45°, as illustrated in Fig. 1. Dissociation of the parent molecules oriented with the transition dipole moment $\vec{\mu}$ more aligned along the laser polarization [Fig. 1(a)] is favored over dissociation of those molecules oriented with the tran-

sition dipole moment more perpendicular to the laser polarization [Fig. 1(b)]. As the permanent dipole $\vec{d}$ has a nonzero angle with the transition dipole moment $\vec{\mu}$,[17] the azimuthal angle of $\vec{d}$ and $\vec{\mu}$ is constrained about the orientation axis for the dissociated molecules only. This implies that the dissociated molecules are effectively three-dimensionally fixed in space. The orientation of the vectors $\vec{d}$, $\vec{\mu}$, $\vec{\epsilon}$, and $\vec{O}$ in the laboratory frame is drawn schematically in Fig. 2(a).

In this paper we present a full report on the experimental results for all populated rotational levels of the CO(J) photofragment from dissociation of oriented OCS molecules. We will address the observed asymmetric spatial distribution in further detail and give a quantitative analysis of our data in terms of molecular frame directional properties. In Sec. II we will discuss the theoretical framework for the analysis of our results. In Sec. III we will briefly describe the experimental setup, and in Sec. IV we will present our data for the full range of rotational states. In Sec. V we will report an extensive analysis and interpretation of the experimental results in relation to quatitative details of the dissociation dynamics in the molecular frame. We will summarize our conclusions in Sec. VI.

II. THEORY

In a previous theoretical paper[23] we derived general and explicit expressions for the photofragment angular recoil distribution $I(\theta)$ after photolysis of an oriented molecule. For convenience we repeat here four equations from Ref. 23 of relevance for the current experimental geometry where we photolyse a symmetric top molecule in a $(JKM)=(J\ell M)=(111)$ state. The spatial distribution $I_{JKM}(\theta_{dO})$ of the permanent dipole moment $\vec{d}$ of the oriented $(J\ell M)$ symmetric top molecule can be written as an expansion of Legendre polynomials P_k,[10]

$$I_{JKM}(\theta_{dO})=\frac{1}{2}+\sum_{k=1}^{2J} c_k P_k(\cos\theta_{dO}), \tag{2}$$

where θ_{dO} is the angle of the permanent dipole moment $\vec{d}$ with the laboratory direction of the dc orientation field $\vec{O}$ [see Fig. 2(a)]. For OCS in the $(\nu_2=1|J\ell M=111)$ state, the expansion coefficients are $c_1=3/4$ and $c_2=1/4$. If the angle Γ between the linear polarization of the dissociation laser and the orientation axis equals 45°, the angular recoil distribution $I(\theta)$ for the outermost ring of the two-dimensional (2D) experimental image can be written as[23]

$$I(\theta)=1+\beta_1 P_1(\cos\theta)+\beta_2 P_2(\cos\theta) \tag{3}$$

with

$$\beta_1=\left(\frac{3c_1\sin\chi\cos\chi\sin\alpha}{[1+2c_2P_2(\cos\alpha)][1-(1/2)P_2(\cos\chi)]+(3/16)c_2\sin^2\chi\sin^2\alpha}\right), \tag{4}$$

$$\beta_2=\left(\frac{[1+2c_2P_2(\cos\alpha)]P_2(\cos\chi)+(3/8)c_2\sin^2\chi\sin^2\alpha}{[1+2c_2P_2(\cos\alpha)][1-(1/2)P_2(\cos\chi)]+(3/16)c_2\sin^2\chi\sin^2\alpha}\right), \tag{5}$$

where θ is the polar angle between the vertical direction and the velocity $\vec{v}$ for the 2D images. The angle between the asymptotic recoil velocity $\vec{v}$ and the permanent dipole $\vec{d}$ of OCS is α, the angle between $\vec{v}$ and the transition dipole moment $\vec{\mu}$ is χ, and the corresponding azimuthal angle is $\varphi_{\mu d}$, as illustrated in Fig. 2(b). The $P_1(\cos\theta)$ Legendre polynomial in Eq. (3) indicates an orientational asymmetry in the laboratory frame recoil distribution perpendicular to the parent molecule orientation axis. The magnitude of this asymmetric contribution is given by β_1. It follows from Eq. (4) that the asymmetry parameter β_1 vanishes for $\chi=0$, $\chi=90°$, or $\alpha=0$. For excitation to the $1\,^1A''$ excited state $\chi=90°$ which means that a pure perpendicular excitation cannot produce a P_1 contribution in the recoil distribution. For a nonzero value of β_1, anisotropy of the scattering potential energy surface(s) is not required: recoil along the axis of a dissociating bond that makes a nonzero angle with both the $\vec{d}$ and $\vec{\mu}$ will always results in an asymmetric laboratory frame spatial distribution for oriented molecules under these experimental conditions. For excitation to the $2\,^1A'$ state we have reported before[20] that $\chi\approx16°$ and excitation to this state can yield a nonzero P_1 contribution. If the angles between the initial C–S bond and $\vec{d}$ and $\vec{\mu}$ are small, for instance, if $\alpha\approx\chi$, we find from Eq. (4) a small $\beta_1\approx0.2$ in the absence of anisotropic forces on the recoiling photofragments. Therefore, a value of β_1 larger than ≈0.2 indicates nonaxial recoil in the photodissociation of OCS.

The rotationally cold channel in the CO(J) rotational distribution is caused by simultaneous excitation to the $2\,^1A'$ and $1\,^1A''$ surfaces. This means that the angular distribution of the cold channel may have some P_1 contribution, but this contribution is caused entirely by the $2\,^1A'$ fraction of the transition. The rotationally hot channel is produced by excitation to the $2\,^1A'$ state only. In this paper, we focus on the rotationally hot channel mainly and refer to $\chi_{2\,^1A'}$ and $\vec{\mu}_{2\,^1A'}$ as χ and $\vec{\mu}$, respectively.

Although not discussed in Ref. 23, rotation of the OCS molecule during the dissociation can have an effect on the spatial recoil distribution. In the case of OCS$(\nu_2=1|J\ell M=111)$, the parent molecule rotates about the OCS symmetry axis, which implies a rotation of $\vec{\mu}$ about $\vec{d}$. Rotation of the dissociating molecule in one direction would change an up-

down asymmetry into a left-right asymmetry (see Figs. 1 and 2). However, the hexapole selects the ($J\ell M=111$) state and the ($J\ell M=-1-1-1$) state simultaneously. OCS in the latter state has the same spatial distribution but rotates in the opposite direction. Therefore, these effects cancel in the measured image. The only way that, in principle, rotation of the OCS parent molecule will affect the experiment is in a decrease of the measured asymmetry β_1. Furthermore, rotation contributes to the azimuthal angle $\varphi_{\mu d}$ because the angle between $\vec{d}$ and $\vec{\mu}$, $\chi-\alpha$, is fixed and $\vec{d}$ is nearly parallel to the direction of the recoiling moieties shortly after the moment of excitation [this corresponds to $\alpha\approx 0$ and $\chi-\alpha\neq 0$ in Fig. 2(b)]. The dependence on $\varphi_{\mu d}$ is accounted for by applying the following substitutions to the equations in Ref. 23:

$$c_1 \sin\chi\cos\chi\sin\alpha \rightarrow c_1 \cos\varphi_{\mu d}\sin\chi\cos\chi\sin\alpha,$$

$$c_2 \sin^2\chi\sin^2\alpha \rightarrow c_2 \cos 2\varphi_{\mu d}\sin^2\chi\sin^2\alpha,$$

$$\pm \rightarrow +,$$

$$\mp \rightarrow -.$$

Application of these replacements to Eqs. (4) and (5) yields the more general expressions,

$$\beta_1=\left(\frac{3c_1\cos\varphi_{\mu d}\sin\chi\cos\chi\sin\alpha}{[1+2c_2P_2(\cos\alpha)][1-1/2P_2(\cos\chi)]+3/16c_2\cos 2\varphi_{\mu d}\sin^2\chi\sin^2\alpha}\right) \tag{6}$$

and

$$\beta_2=\left(\frac{[1+2c_2P_2(\cos\alpha)]P_2(\cos\chi)+3/8c_2\cos 2\varphi_{\mu d}\sin^2\chi\sin^2\alpha}{[1+2c_2P_2(\cos\alpha)][1-1/2P_2(\cos\chi)]+3/16c_2\cos 2\varphi_{\mu d}\sin^2\chi\sin^2\alpha}\right). \tag{7}$$

The asymptotic value of $\varphi_{\mu d}$ cannot be determined explicitly as there are three unknowns (α, χ, and the additional $\varphi_{\mu d}$) in the two Eqs. (6) and (7). This will be addressed below in the Discussion section.

The excitation via the Q branch to the resonant intermediate during the CO(J) ionization is not very sensitive to the polarization of the laser,[16] so Eqs. (3)–(5) are used for interpretating CO(J) angular distributions without further complications from rotational alignment effects.

III. EXPERIMENT

The experimental setup has been described in more detail before.[14,20] The electrostatic lens used in the original setup was replaced by a velocity map ion lens.[24] A skimmed molecular beam (20% OCS in Ar) is directed through a hexapole which focuses OCS molecules in the ($\nu_2=1|J\ell M=111$) state on a collimator in the repeller plate of the ion lens. The molecular beam hits a beam stop 10 cm upstream from the hexapole entrance, which enhances the selectivity of the hexapole.[20] The OCS($\nu_2=1|J\ell M=111$) molecules are oriented in the extraction field of the electrostatic lens, which has a strength of about 200 V/cm. The state-selected molecular beam is intersected perpendicularly by a linearly polarized frequency doubled tunable dye laser with a wavelength around 230 nm. The angle between the polarization axis of the laser and the molecular beam propagation direction is set at 45° [see also Fig. 1(a) in Ref. 22]. The 230 nm laser dissociates the OCS molecules into S($^1D_2$) and CO(J) fragments and subsequently state-selectively ionizes the nascent CO(J) photofragments in a (2+1) resonantly enhanced multiphoton ionization (REMPI) scheme via the $B\,^1\Sigma^+$ intermediate state. The laser beam is focused by a lens with a focal length of 20 cm, which was positioned ~1.5 cm out of focus to avoid line broadening of the CO(J) Q-branch rotational spectrum. The CO^+ photofragment ions are velocity mapped on a Micron-Channel-Plate/phosphor screen detector which is gated to detect only the $m/e=+28$ ions. The laser wavelength is scanned over the Doppler profile of each of the rotational lines in the $B\,^1\Sigma^+ \leftarrow\leftarrow X\,^1\Sigma^+$ Q branch, while the charge coupled device (CCD) camera collected the phosphor screen luminescence signal.

IV. RESULTS

A raw data image of the CO($v=0,J=63$) photofragment after OCS photolysis at 230 nm is shown in Fig. 3(a). A strong up-down asymmetry can be observed. In our experiments, we make use of ''conventional'' velocity mapping in the sense that the projection of the full 3D ion sphere is

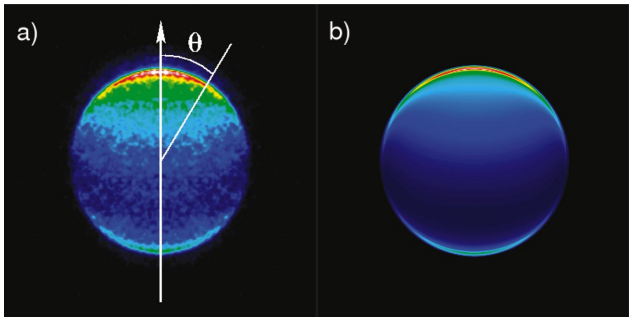

FIG. 3. (Color) (a) Typical raw data image of CO($v=0,J=63$) after OCS($\nu_2=1|J\ell M=111$) photolysis in the symmetry breaking geometry of orientation and photolysis direction. Regions with red/white have the largest intensity, regions with blue/black have the smallest intensity. The up-down asymmetry, which is strongest in the outermost ring, is clearly visible. (b) Simulated data image obtained by projecting the theoretical 3D ion distribution onto a 2D plane and convoluting the projection with a Gaussian mask. The angles χ and α were set to 162° and 133°, respectively. As in the experimental data, the strongest up-down asymmetry is observed in the outer ring of the image.

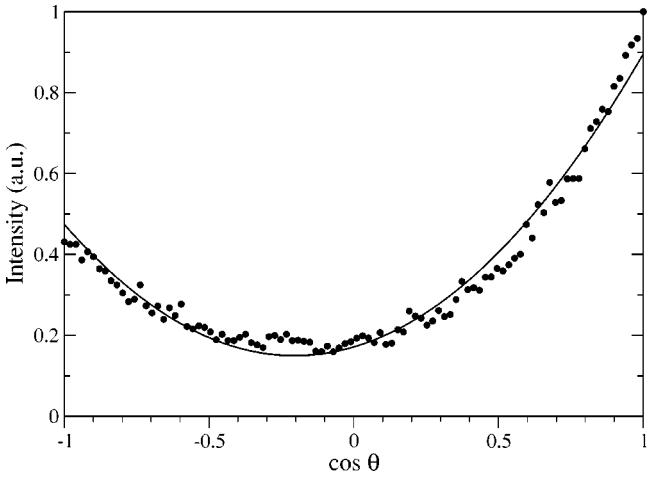

FIG. 4. Angular distribution of the outer ring of the image in Fig. 3(a), showing a strong up-down asymmetry. The solid line is the fit of Eq. (3) to the experimental data.

measured. Equations (3)–(5) are derived[23] for a 2D cut through the real 3D distribution obtained by for instance slice imaging.[25] Nevertheless, we can use Eqs. (4) and (5) to extract the β_1 and β_2 coefficients from our data by analyzing only the outer ring of the projection, as this part corresponds to the ions which recoil perpendicular to the time-of-flight (TOF) axis. The outcome of the analysis is somewhat sensitive to the chosen radial range and to a lower degree to the subtracted background. Therefore, although the data is not Abel invertible, we use the velocity distribtution of the Abel inverted image to systematically determine the radial range of the outer ring of the raw data for which the angular distribution will be extracted. The angular distribution of this range of the raw data image shown in Fig. 3(a) is fitted using Eq. (3) and plotted in Fig. 4. A simulated data image, obtained by projecting the calculated 3D distribution onto a 2D plane [see Eq. (11) of Ref. 23] is shown in Fig. 3(b). The simulated image was convoluted with a Gaussian mask to incorporate the apparatus function. For simulating the data image, the angles χ and α were set at 162° and 133°, respectively. These molecular frame angles give $\beta_1=0.77$ and $\beta_2=1.46$, in good agreement with the experimental data for $J=63$, see Table I. Clearly, the theoretical image resembles the experimentally observed image, indicating that the theoretical model we derived supports the analysis.[23] The fitted β_1 and β_2 values for each of the populated CO(J) rotational states J are plotted in Fig. 5, and are denoted in Table I. The error bars are obtained from three experimental images at each J state and represent 1σ. For the rotationally cold channel ($J\leqslant 57$), a significantly lower β_1 amplitude is observed compared to the hot channel ($J\geqslant 58$). A similar trend is observed for the β_2 distribution. Furthermore, we have derived[23] that $\beta_1 \propto \sin(2\Gamma)$, where Γ is the angle between the laser polarization and the detection axis. This means that the asymmetric recoil distribution can only be observed when $\Gamma\neq 0$ and $\Gamma\neq 90°$, and β_1 is maximal when $\Gamma=45°$. For CO($J=50$), the variation of the measured β_1 with changing polarization angle Γ is shown in Fig. 6. We clearly observe $\beta_1 \propto \sin(2\Gamma)$, in accordance with the theory.[23]

TABLE I. The β_1 and β_2 values obtained from the outer rings of the experimental CO(J) data images from OCS($\nu_2=1|J\ell M=111$) photolysis at 230 nm. The denoted standard deviation (1σ) is directly calculated from three independent measurements at each CO(J) state.

J	β_1	β_2
47	0.40±0.04	0.53±0.01
48	0.42±0.08	0.57±0.02
49	0.21±0.25	0.62±0.03
50	0.28±0.04	0.59±0.03
51	0.36±0.10	0.60±0.01
52	0.42±0.08	0.70±0.01
53	0.31±0.09	0.70±0.03
54	0.30±0.05	0.68±0.04
55	0.32±0.02	0.81±0.10
56	0.41±0.03	0.99±0.04
57	0.32±0.02	0.88±0.05
58	0.67±0.02	1.23±0.07
59	0.54±0.13	1.27±0.02
60	0.68±0.04	1.48±0.03
61	0.70±0.13	1.57±0.03
62	0.71±0.06	1.58±0.05
63	0.73±0.02	1.49±0.02
64	0.71±0.15	1.32±0.08
65	0.95±0.05	1.30±0.01

As the CO recoil distribution is strongly asymmetric such an asymmetry should also be observable in the angular recoil of the S($^1D_2$) cofragment. A data image of the S($^1D_2$) cofragment is shown in Fig. 7. To obtain this image the photolysis laser beam at 230 nm propagated top down, with its linear polarization at 45° with the TOF axis. The S($^1D_2$) photofragment was ionized by a second, circularly polarized, laser at 291.48 nm using a (2+1) REMPI scheme via the $^1P_1$ intermediate.[26] The apparent tilted angular distribution (maximum intensity around 135°, 270° clockwise to the vertical) is caused by polarization of the S($^1D_2$) orbital due to interference of simultaneously excited potential energy surfaces.[26] This tilt, observed by using the circularly polarized probe laser, is outside the scope of the present paper and quantitative results on the polarization of S($^1D_2$) will be published later. Besides the tilt, we also observe an inversion (left-right) asymmetry in the S($^1D_2$) laboratory frame recoil

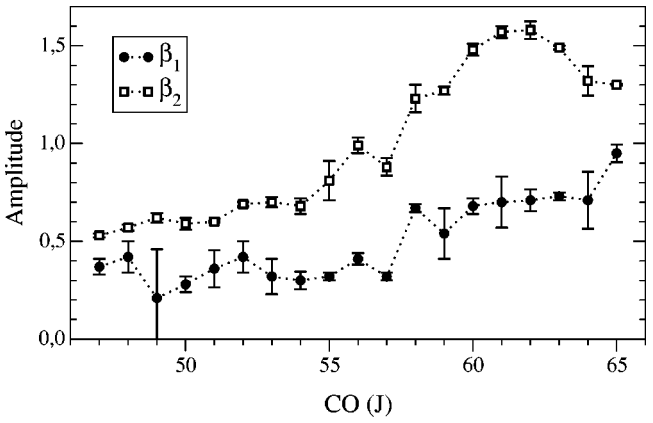

FIG. 5. The β_1 and β_2 amplitudes [see Eq. (3)] as observed for each CO(J) rotational state after OCS($\nu_2=1|J\ell M=111$) photolysis at 230 nm. The slow and fast channel can approximately be distinguished where β_1 changes abruptly at $J\approx 58$.

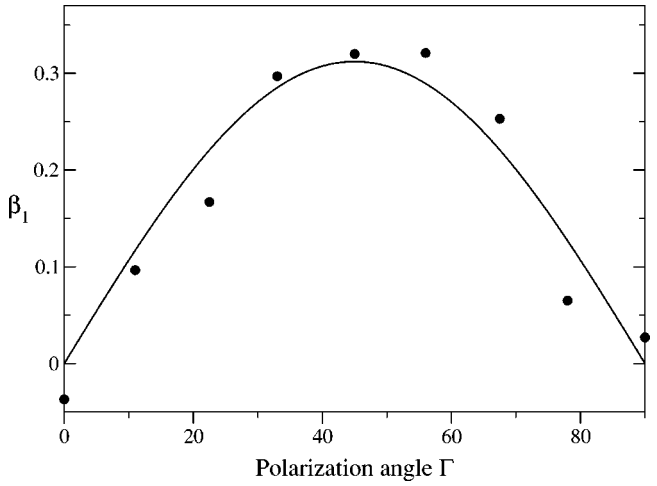

FIG. 6. The β_1 amplitude, in this case for CO($J=50$), as a function of the angle Γ between the laser polarization and the orientation axis. A sin(2Γ) dependence of β_1 is observed, demonstrating the modulation of the asymmetry with the photolysis polarization geometry. For comparison a fitted $\beta_1(\Gamma)=\beta_{1,\max}\sin(2\Gamma)$ is plotted as a solid line.

distribution. In the S($^1D_2$) image, the slower S-fragment channel (correlating with CO cofragments in high J states) and the faster S-fragment channel (correlating with CO cofragments in low J states) are well separated. Note how in the slow channel at smaller radii rings are visible corresponding to discrete velocity bands of the S atom because of total energy conservation and the quantized energy spacings of the rotationally highly excited CO cofragment. It is found from analysis of the S($^1D_2$) images that the slow channel is strongly asymmetric whereas the fast channel is more weakly asymmetric. This is fully consistent with the higher β_1 values we observed for the high J channel compared to the lower β_1 values for the low J channel (see Table I and Fig. 5).

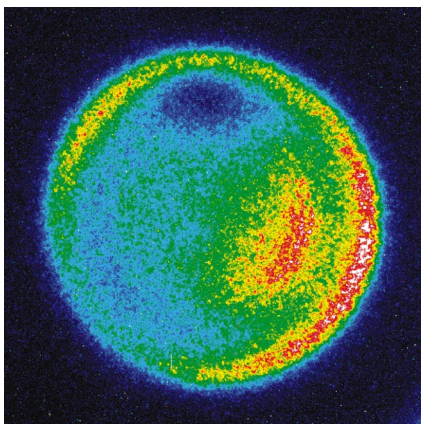

FIG. 7. (Color) Raw data image of the S($^1D_2$) photofragment after photolysis at 230 nm and a second probe laser to detect S($^1D_2$). The slow channel is more asymmetric than the fast channel, in accordance with the higher β_1 we observed for the high J states of the angular distribution of the CO(J) cofragment in Fig. 5.

V. DISCUSSION

The state-selected OCS($\nu_2=1|J\ell M=111$) parent molecule is oriented by a positive Stark effect, which means that the permanent dipole moment $\vec{d}$ points opposite to the direction of the orientation field $\vec{O}$. Equation (2) describes the orientation probability distribution of the linear symmetry axis of the parent molecule in the electric field. The saturation parameter S,[27,28] of uncoupling the ℓ doubling from the ($J\ell M=111$) wave function in the extraction field of the ion lens $\vec{E}$ was calculated to be 0.984 and the corresponding average $\langle\cos(\vec{E}\cdot\vec{d})\rangle=0.492$, where the maximum value equals $\ell M/J(J+1)=0.5$.[10] This means that the ($\nu_2=2|J\ell M=111$) state-selected molecules are practically completely oriented with the S atom pointing towards the positively charged repeller.

As the rotational motion of the parent molecule is induced by excitation of the degenerate bending vibration,[28] the rotational period can be estimated to be 64 fs using the vibrational frequency of 520.4 cm^{-1}.[19] Due to strong bending of the dissociating molecule on the anisotropic excited potential energy surface and the increasing distance between the S and CO moieties,[17] the moment of inertia of the molecule will increase rapidly during the dissociation slowing down the rotation of the dissociating molecule. As $\varphi_{\mu d}$ rotates $\vec{\mu}$ about $\vec{v}$ [see Fig. 2(b)], the small value of χ we observed indicates that the asymptotic recoil velocity $\vec{v}$ is hardly affected by the parent molecule rotation. Therefore, the effect on β_1 will be limited, although the value of α we extract from the observed β_1 may be somewhat smaller than the real value. In order to measure the exact value of $\varphi_{\mu d}$ additional experiments using a pump-probe laser geometry which is more sensitive to $\varphi_{\mu d}$ at small values of χ are required. In a geometry in which the laser polarization is parallel to the orientation field and the detector plane, which corresponds to $\Gamma=\Delta=90°$ (in the formalism described in Ref. 23), since $\vec{d}$ is nearly parallel to the C–S axis, the angular distribution is more sensitive to $\varphi_{\mu d}$ at small values of χ. The geometry in which the molecules are oriented horizontally, and photolyzed by a vertically polarized laser (i.e., $\Gamma=90°$ and $\Delta=0$), as applied in Ref. 20, has no or a negligible dependence on $\varphi_{\mu d}$. In light of the arguments above we use Eqs. (4) and (5) for the present analysis.

As pointed out before,[23] the β_2 value can directly be used to extract the value of χ, as β_2 depends on the value of α only to a very small extent. From the highest β_2 value (see Table I $\beta_2=1.58$, for $J=62$; note this is for a different J state than the image presented in Fig. 3), we find $\chi=164\pm1°$, in accordance with the 16° (=180°−164°, see discussion below) obtained by measuring the conventional β parameter directly.[20] Using $\chi=164°$ and $\beta_1=0.71$ we find $\alpha=133\pm3°$. These values are in good agreement with those obtained by fitting β_1 and β_2 of the outer ring of a simulated data image, which yields $\chi=167°$ and $\alpha=135°$.[22] This indicates that the analysis of the outer ring of the 2D projected and convoluted data is consistent with our theoretical model. The values of β_1 and β_2 for $J=62$ reported before,[22] were obtained using a slightly different radial range and background subtraction in extracting the angular distribution of the outer ring, lead-

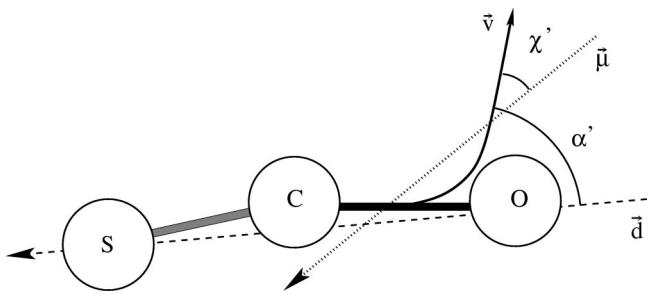

FIG. 8. Schematic overview of the vector correlations in the photodissociation of OCS after excitation to the $2\,^1A'$ potential energy surface. χ' and α' are the deflection angles of the recoiling photofragment velocity with respect to $-\vec{d}$ and $-\vec{\mu}$ (see text). Due to the anisotropic potential energy surface the dissociation proceeds along a curved trajectory (solid line). The recoiling photofragments bend away from the permanent dipole $\vec{d}$ and the final recoil velocity passes beyond the transition dipole moment $\vec{\mu}$.

ing to only marginally different values from those reported here. This, however, does not affect the interpretation of the data.

From the observed β_1 and β_2, we obtain the angles $\chi=164°$ and $\alpha=133°$. Both $\vec{d}$ and $\vec{\mu}$ point toward the S atom rather than toward the O atom. Defining α' and χ' as the polar angles of $\vec{v}$ with respect to $-\vec{d}$ and $-\vec{\mu}$, respectively, yields $\alpha'=180°-\alpha=47°$ and $\chi'=180°-\chi=16°$. This allows a more convenient interpretation of χ' and α' as the deflection angles of the recoiling photofragment with respect to $-\vec{d}$ and $-\vec{\mu}$. Note that in case of S($^1D_2$) detection, α and χ themselves would apply as deflection angles. Considering the obtained values for α, χ, and the positive β_1, $\vec{d}$ and $\vec{\mu}$ must be on the same side of $\vec{v}$. The corresponding physical interpretation is that since $\vec{d}$ is nearly parallel to the C–S axis, during the dissociation, the recoiling photofragments bend away from the permanent dipole moment $\vec{d}$. As the angle between $\vec{d}$ and $\vec{v}$ is larger than the angle between $\vec{\mu}$ and $\vec{v}$, and $\vec{d}$ and $\vec{\mu}$ are on the same side of $\vec{v}$, the recoil direction must even sweep through the direction of the transition dipole moment $\vec{\mu}$ and end up at a small angle of about 16° at the other side of $\vec{\mu}$. This picture is schematically shown in Fig. 8.

An alternative solution for the observed β_1 and β_2 is $\alpha=47°$, $\chi=16°$, defined with respect to $+\vec{\mu}$ and $+\vec{d}$, and $\varphi_{\mu d}=180°$. This solution implies a deflection of 133° with respect to $\vec{d}$. Such a large deflection angle would require a very strong bending on the excited potential energy surface, mainly prior to C–S bond fission. Following *ab initio* calculations presented by Suzuki *et al.*,[17] the C–S distance increases immediately after excitation to the scattering energy surfaces, making a large deflection angle unlikely. Moreover, the angle between $\vec{\mu}$ and $\vec{d}$ would be ~63° for this alternative scenario. We estimated before[20] the angle between the *initial* recoil velocity and the transition dipole moment at ~16°, for a Jacobi angle of 10°, so the angle between $\vec{\mu}$ and $\vec{d}$ is ~26°, in good agreement with the angle obtained from $\alpha'-\chi'=47-16=31°$. Therefore, we feel that the physical picture, as drawn in Fig. 8, is almost certainly the correct interpretation. The direction of the CO(J) photofragment rotational motion is expected to be opposite for the two scenarios, so measurements that are sensitive to the direction of the CO(J) rotation will, in principle, be able to support our conclusion.

As pointed out in Sec. II, only the parallel excitation to the $2\,^1A'$ scattering energy surface will contribute to the β_1 parameter, whereas for the β_2 parameter, both the $2\,^1A'$ and $1\,^1A''$ surfaces can contribute, so, conversely, the experimentally observed parameter β_2 can be split into a parallel and a perpendicular component for each rotational level J,

$$\beta_1(J)=C_\parallel\beta_{1,\parallel}(J,\alpha_\parallel,\chi_\parallel), \tag{8}$$

$$\beta_2(J)=C_\parallel\beta_{2,\parallel}(J,\alpha_\parallel,\chi_\parallel)+C_\perp\beta_{2,\perp}(J,\alpha_\perp,\chi_\perp=90°). \tag{9}$$

Here, $C_\parallel$ and $C_\perp$ are the relative contributions of the parallel transition to the $2\,^1A'$ surface and the perpendicular transition to the $1\,^1A''$ surface, respectively, and $C_\parallel+C_\perp=1$. Note that the missing term $C_\perp\beta_{1,\perp}(J,\alpha_\perp,\chi_\perp=90°)$ in Eq. (8) vanishes because $\beta_1=0$ for $\chi=90°$ [see Eq. (6)]. The two equations, Eqs. (8) and (9), have four unknowns, $\alpha_\parallel$, $\alpha_\perp$, $\chi_\parallel$, and $C_\parallel$ (with $\chi_\perp=90°$ and $C_\perp=1-C_\parallel$), so we have to make some approximations to reduce the number of unknowns to two, in order to solve the system of two equations. First, we notice from Eq. (7) that β_2 depends only weakly on α, varying only 13% about the average value of β_2 over the full range of α (for $\chi=90°$; for smaller values of χ the variation is even smaller). Assuming that the dynamics on both $2\,^1A'$ and $1\,^1A''$ surfaces are not entirely different, we can set $\alpha_\parallel=\alpha_\perp$, to reasonable approximation. Second, we see from Fig. 8 that $|\alpha_\parallel-\chi_\parallel|$ is equal to the angle between $\vec{d}$ and $\vec{\mu}_\parallel$, which equals 31° on average for $J=62$, as mentioned earlier. As $\vec{d}$ and $\vec{\mu}_\parallel$ are vectors in the parent molecular frame, which vary only a few degrees about their average directions, we can assume the angle between them will be approximately constant for all J. Therefore, we use $\chi_\parallel-\alpha_\parallel=31°$ for all J. Using these approximations, we reduce the unknown variables to $\alpha_\parallel$ and $C_\parallel$ and we can solve the system of Eqs. (8) and (9) for these two variables. The obtained deflection angles $\alpha'(=\alpha_\parallel\approx\alpha_\perp)$ and coefficients for the parallel transition $C_\parallel$ are listed in Table II. It appears that the deflection angle α' depends on the rotational state of the CO(J) photofragment only to a small extent. In accordance with conclusions of Suzuki and co-workers[17,21] the low J channel follows from simultaneous excitation of both $2\,^1A'$ and the $1\,^1A''$ scattering energy surfaces, whereas the high J channel follows from excitation of the $2\,^1A'$ state only. Therefore, we believe that the observed change in β_1 as a function of J is caused by a strong change in $2\,^1A'/1\,^1A''$ branching rather than a change in dynamics. It would be highly informative to do semiclassical quantum calculations of the angular recoil distribution from photodissociation of a single ($J\ell M$) state selected OCS parent molecule to compare the experimental results with state-of-the-art theoretical calculations.

VI. CONCLUSIONS

We have experimentally observed the molecular frame directional deflection of photofragments in the photodissociation of laboratory oriented OCS molecules. The photolysis polarization was set at 45° with the orientation axis to inten-

TABLE II. Contributions of the parallel transition from the $1\,^1A'$ ground state to the $2\,^1A'$ excited state $C_\parallel$ relative to the perpendicular transition to the $1\,^1A''$ excited state ($C_\perp = 1 - C_\parallel$), for each J level. The corresponding deflection angle α' is denoted as well. The denoted standard deviation (1σ) is obtained from three independent measurements.

J	$C_\parallel$	α'
47	0.50±0.02	49±2
48	0.52±0.03	49±4
49	0.48±0.08	41±9
50	0.48±0.01	44±2
51	0.51±0.04	47±3
52	0.57±0.03	48±3
53	0.54±0.04	45±3
54	0.52±0.01	44±2
55	0.57±0.05	44±1
56	0.68±0.02	45±1
57	0.60±0.02	43±1
58	0.86±0.03	49±1
59	0.82±0.04	45±1
60	0.95±0.01	47±1
61	0.99±0.06	47±2
62	0.99±0.04	47±1
63	0.97±0.01	48±1
64	0.90±0.08	49±3
65	0.98±0.02	52±1

tionally break the cylindrical symmetry to observe directional asymmetry in the angular recoil distribution. Applying this experimental approach effectively fixes the orientation of the dissociated parent molecules three dimensionally in space. The observed deflection angle of the asymptotic recoil velocity $\vec{v}$ with respect to the permanent dipole moment $\vec{d}$ equals about 47°, larger than the deflection angle with respect to the transition dipole moment $\vec{\mu}$, which equals about 16°. The corresponding physical interpretation is that the recoil velocity bends away from the permanent dipole moment and sweeps through the transition dipole moment. Also, the relative contributions of the two accessible scattering potential energy surfaces on the photodynamics are resolved for each populated CO(J) rotational level, showing a mixed parallel and perpendicular transition corresponding to the low J channel and a pure parallel transition corresponding to the high J channel.

ACKNOWLEDGMENTS

This research was financially supported by the councils for Chemical Sciences and Physical Sciences of the Dutch Organization for Scientific research (NWO-CW, NWO-FOM/Program Molecular Atmospheric Processes). The authors would like to thank J. van Heyst for assistance during the experiments and Professor S. Stolte for support. T.P.R. thanks the EU for support to access the experimental facilities of the Laser Center Vrije Universiteit through the EU program under Contract No. HPRI-CT-1999-00064. A.J.B. thanks the EU for support as a Marie Curie Training Institute fellow at IESL-FORTH under Contract No. HPMT-CT-2000-00201.

[1] R. N. Zare and D. R. Herschbach, Proc. IEEE **51**, 173 (1963).
[2] G. E. Bush and K. R. Wilson, J. Chem. Phys. **56**, 3638 (1972).
[3] S. Yang and R. Bersohn, J. Chem. Phys. **61**, 4400 (1974).
[4] M. D. Morse, Y. Band, and K. F. Freed, J. Chem. Phys. **78**, 6066 (1983).
[5] R. Schinke, *Photodissociation Dynamics* (Cambridge University Press, Cambridge, 1995).
[6] E. Wrede, E. R. Wouters, M. Beckert, R. N. Dixon, and M. R. N. Ashfold, J. Chem. Phys. **116**, 6064 (2002).
[7] G. Balint-Kurti and M. Shapiro, Chem. Phys. **61**, 137 (1981).
[8] C. A. Taatjes, M. H. M. Janssen, and S. Stolte, Chem. Phys. Lett. **203**, 363 (1993).
[9] T. Seideman, J. Chem. Phys. **102**, 6487 (1995).
[10] S. E. Choi and R. B. Bernstein, J. Chem. Phys. **85**, 150 (1986).
[11] R. N. Zare, Chem. Phys. Lett. **156**, 1 (1989).
[12] T. Seideman, Chem. Phys. Lett. **253**, 279 (1996).
[13] J. W. G. Mastenbroek, C. A. Taatjes, K. Nauta, M. H. M. Janssen, and S. Stolte, J. Phys. Chem. **99**, 4360 (1995).
[14] M. H. M. Janssen, J. W. G. Mastenbroek, and S. Stolte, J. Phys. Chem. A **101**, 7605 (1997).
[15] N. Sivakumar, G. E. Hall, P. L. Houston, J. W. Hepburn, and I. Burak, J. Chem. Phys. **88**, 3692 (1988).
[16] Y. Sato, Y. Matsumi, M. Kawasaki, K. Tsukiyama, and R. Bersohn, J. Phys. Chem. **99**, 16307 (1995).
[17] T. Suzuki, H. Katayanagi, S. Nanbu, and M. Aoyagi, J. Chem. Phys. **109**, 5778 (1998).
[18] Z. H. Kim, A. J. Alexander, and R. N. Zare, J. Phys. Chem. A **103**, 10144 (1999).
[19] A. Sugita, M. Mashino, M. Kawasaki, Y. Matsumi, R. Bersohn, G. Trott-Kriegeskorte, and K.-H. Gericke, J. Chem. Phys. **112**, 7095 (2000).
[20] A. J. van den Brom, T. P. Rakitzis, J. van Heyst, T. N. Kitsopoulos, S. R. Jezowski, and M. H. M. Janssen, J. Chem. Phys. **117**, 4255 (2002).
[21] H. Katayanagi and T. Suzuki, Chem. Phys. Lett. **360**, 104 (2002).
[22] T. P. Rakitzis, A. J. van den Brom, and M. H. H. Janssen, Science **303**, 1852 (2004).
[23] T. P. Rakitzis, A. J. van den Brom, and M. H. M. Janssen, Chem. Phys. Lett. **372**, 187 (2003).
[24] A. T. J. B. Eppink and D. H. Parker, Rev. Sci. Instrum. **68**, 3477 (1997).
[25] C. R. Gebhardt, T. P. Rakitzis, P. C. Samartzis, V. Ladopoulos, and T. N. Kitsopoulos, Rev. Sci. Instrum. **72**, 3848 (2001).
[26] T. P. Rakitzis, P. C. Samartzis, and T. N. Kitsopoulos, J. Chem. Phys. **111**, 10415 (1999).
[27] J. M. L. J. Reinartz, W. L. Meerts, and A. Dynamus, Chem. Phys. Lett. **16**, 576 (1972).
[28] C. H. Townes and A. L. Schawlow, *Microwave Spectroscopy* (McGraw-Hill, New York, 1955).